Supplementary Information

for

Effects of natural organic matter and sulfidation on the flocculation and filtration of silver nanoparticles

Tongren Zhu[a], Desmond F. Lawler[a*], Yunqi Chen[b] and Boris L. T. Lau[b*]

* Corresponding authors
[a]Dept. of Civil, Architectural & Environmental Engineering, University of Texas; One University Station C1786; Austin, TX USA dlawler@mail.utexas.edu; phone 01 512 471 4595; fax 01 512 471 0592
[b]Dept. of Civil & Environmental Engineering, 130 Natural Resources Road, University of Massachusetts, Amherst, MA 01003 USA; borislau@umass.edu; phone 01 413 545 5423; fax 01 413 577 4940

Linearized superposition approximation (LSA) could yield simple analytical expressions for the electrostatic repulsion without encountering the inconvenient numerical calculations that stem from various boundary conditions (i.e., constant surface charge or constant surface potential). The results based on LSA fall in between those based on constant surface charge and constant surface potential, the two extremes of interparticle interaction.[1] Therefore, analytical expressions based on LSA were used to calculate electrostatic repulsion.

Van der Waals (vdW) attraction can be calculated as a pairwise summation of all the relevant interactions between molecules in the two interacting bodies. The approximate analytical expressions from John Gregory (1981) yielded good fit to exact computations to account for the retardation effect.[2] Thus, the approximate expressions by John Gregory were used to quantify the vdW attraction.

The expressions for the steric hindrance are more semi-quantitative due to various assumptions and the limitation in getting values of parameters. Nevertheless, analytical expressions by Vincent et. al. (1986) for particle-particle interaction and by Lin and Wiesner (2012) for particle-collector interaction have been widely used.[3,4] These expressions are conceptually rigorous and could provide insight to the effect of steric hindrance.

Table S1. Equations to calculate particle-particle and particle-collector interactions

Types	Geometry	Equation	Reference
Electrostatic repulsion	Particle-particle	$V_R = 32\pi\varepsilon_0\varepsilon_r a_1\left(\frac{k_BT}{ze}\right)^2\left[tanh\left(\frac{ze\psi_1}{4k_BT}\right)\right]^2 e^{-\kappa h}$	5
	Particle-collector	$V_R = 32\pi\varepsilon_0\varepsilon_r a_1\left(\frac{k_BT}{ze}\right)^2 tanh\left(\frac{ze\psi_1}{4k_BT}\right) tanh\left(\frac{ze\psi_2}{4k_BT}\right) e^{-\kappa h}$	
Van der Waals attraction	Particle-particle	$V_A = -\frac{A_{131}a_1}{12h}\left(1 + \frac{14h}{\lambda}\right)^{-1}$	2
	Particle-collector	$V_A = -\frac{A_{132}a_1}{6h}\left(1 + \frac{14h}{\lambda}\right)^{-1}$	
Steric hindrance	Particle-particle ($h < \delta$)	$V_{S,mix} = \frac{4\pi a_1 k_BT}{v_S}\Phi^2\left(\frac{1}{2} - \chi\right)\delta^2\left[\frac{h}{2\delta} - \frac{1}{4} - ln\left(\frac{h}{\delta}\right)\right]$ $V_{S,el} = \frac{2\pi a_1 k_BT\delta^2\rho\Phi}{MW}\left\{\frac{h}{\delta}ln\left[\frac{h}{\delta}\left(\frac{3 - \frac{h}{\delta}}{2}\right)^2\right] - 6ln\left(\frac{3 - \frac{h}{\delta}}{2}\right) + 3\left(1 - \frac{h}{\delta}\right.\right.$	3
	Particle-particle ($\delta < h < 2\delta$)	$V_{S,mix} = \frac{4\pi a_1 k_BT}{v_s}\Phi^2\left(\frac{1}{2} - \chi\right)\left(\delta - \frac{h}{2}\right)^2$, $V_{S,el} = 0$	
	Particle-collector ($h < \delta$)	$V_{S,mix} = k_BT\left(\frac{{V_P}^2}{v_S}\right)\left(\frac{1}{2} - \chi\right)\Phi^2 V_{1,S}\left(\frac{V_{1,S}}{V_3} - 1\right)$ $V_{S,el} = k_BT\gamma\delta^2\pi(1 - \hbar)(2\tilde{a}_1 + \hbar - 1)ln\left[\frac{3(2\tilde{a}_1 + \hbar - 1)}{\hbar^2 + 3\hbar\tilde{a} + \hbar + 3\tilde{a} -}\right.$	4
		$V_S = V_{S,mix} + V_{S,el}$	
Total XDLVO		$V_{total} = V_R + V_A + V_S$	

Table S2. Parameters used in the calculation of XDLVO energy of interactions

Parameter	Values or definition
ε_0	Permittivity in vacuum, 8.854×10-12 C^2/J-m
ε_r	Relative permittivity of water, 78.5
a_1	Radius of the particle
k_B	Boltzmann constant, 1.38×10^{-23} J/K
T	Absolute temperature, 298 K
z	Valence of electrolytes, 1 for $NaNO_3$
e	Elementary charge, 1.602×10^{-19} C
ψ_1	Surface potential of the particle from Table 1
κ	Inverse debye length, $\kappa = \sqrt{\frac{1}{\varepsilon_0 \varepsilon_r kT}\sum_{i=1}^{M} {z_i}^2 e^2 n_i^\infty}$ where ionic strength is 10 mM $NaNO_3$ for self-aggregation and 5 mM $NaNO_3$ for deposition
h	Surface-surface separation distance
ψ_2	Surface potential of the column granular media (-65 mV) and the QCM quartz sensor (-33 mV)[6]
A_{131}	Hamaker constant of particle-particle interaction in water, $A_{131} = (\sqrt{A_{11}} - \sqrt{A_{33}})^2$, Hamaker constant of AgNP (A_{11}=1.5×10^{-19} J)[7], and Hamaker constant of water (A_{33}=4×10^{-20} J)[8]
A_{132}	Hamaker constant of particle-collector interaction in water, $A_{132} = (\sqrt{A_{11}} - \sqrt{A_{33}})(\sqrt{A_{22}} - \sqrt{A_{33}})$, Hamaker constant of silica (A_{22}=6.5×10^{-20} J)[8]
λ	Characteristic wavelength, 100 nm
v_S	Molecular volume of solvent, 0.03 nm
Φ	Polymer segment density, 0.1 for PVP-AgNPs, 0.05 for HA-AgNPs, 0 for S-AgNPs, and 0.01 for HA-S-AgNPs
χ	Flory-Huggins parameter, 0.45 in a good solvent
δ	Capping layer thickness, 5 nm
ρ	Density of polymer (1 g/mL)
MW	Molecular weight of polymer, 40000 for PVP, 3310 for HA[9]
V_P	Molecular volume of polymer
$V_{1,S}$	Dimensionless volumes of compression domain defined by Eq. 22' in Lin and Wiesner (2012)[4]
V_3	Dimensionless volumes of compression domain defined by Eq. 24' in Lin and Wiesner (2012)[4]
γ	Number of polymer anchoring site per area, defined by Eqs. 17 and 18 in Lin and Wiesner (2012)[4]
$\tilde{h}$	Dimensionless distance, h/δ
$\tilde{a}_1$	Dimensionless radius, a_1/δ
$V_{S,\,mix}$	Steric hindrance from osmotic contribution
$V_{S,\,el}$	Steric hindrance from electric contribution

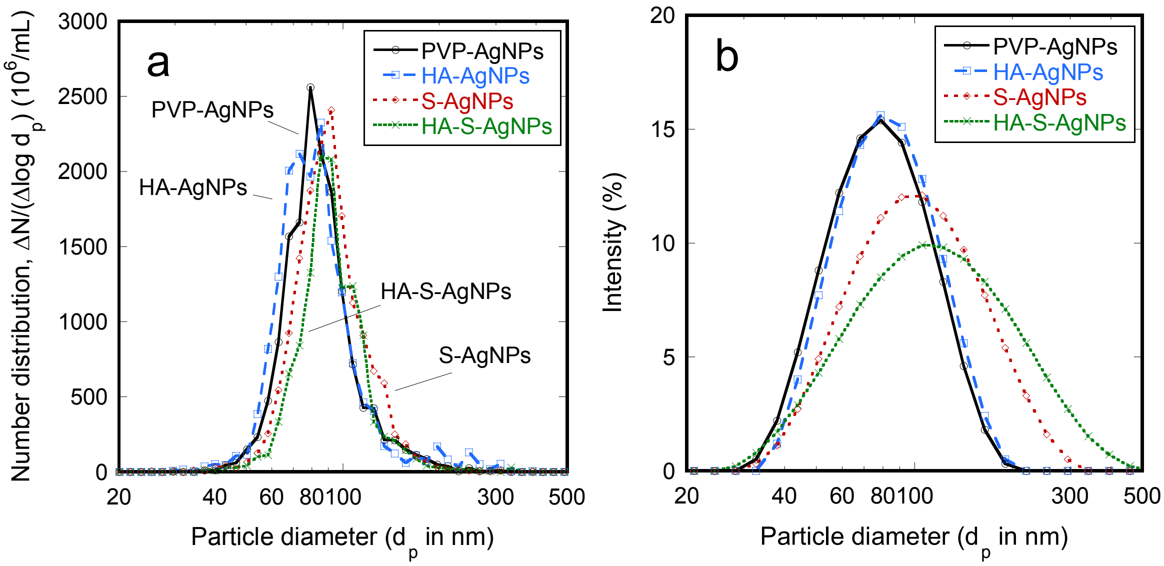

Figure S1. Hydrodynamic diameter distribution by a) NTA, and b) DLS under different transformations at pH=7.0±0.2 and I=5 mM $NaNO_3$.

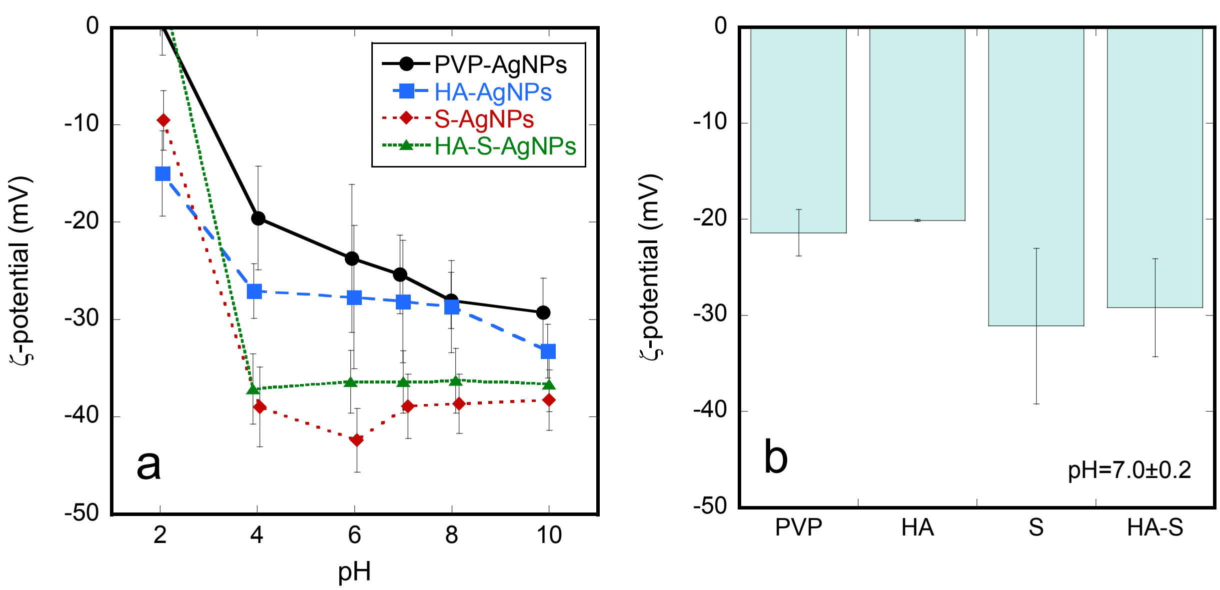

Figure S2. ζ potential by a) EPM, and b) ELS under different transformations at I=5 mM $NaNO_3$.

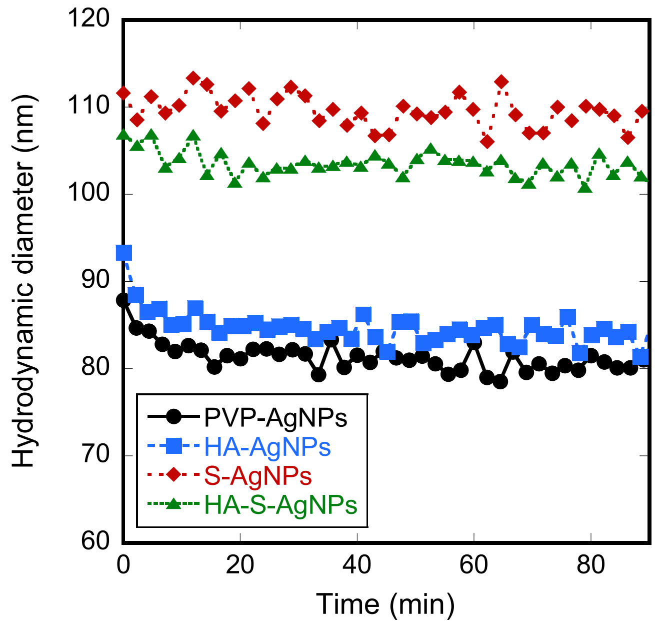

Figure S3. The hydrodynamic diameter of AgNPs under different environmental transformations at pH=7.0±0.2 and I=5 mM $NaNO_3$.

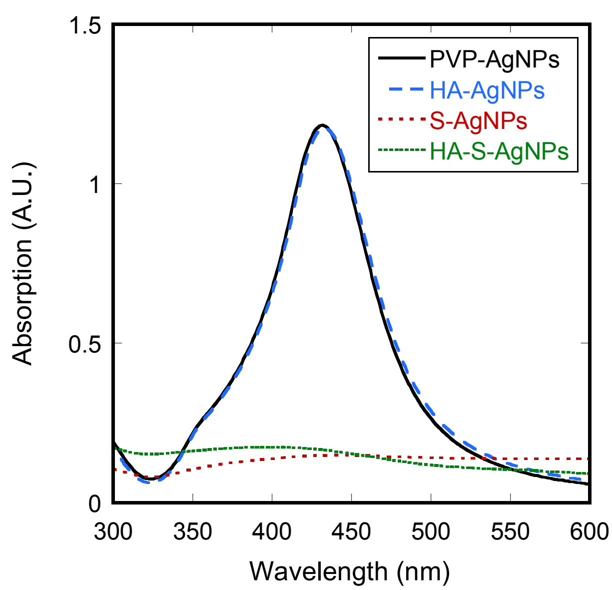

Figure S4. UV-vis absorption spectra of PVP-AgNPs under environmental transformation

The distinct absorption peaks at around 435 nm wavelength were measured by a UV-vis spectrophotometer to visualize the change of the metallic silver before and after transformation. Exposure of the PVP-AgNPs to HA did not result in the oxidation of the metallic silver or an increased particle size. Sulfidation changed the color of the AgNPs suspension from orange to black with the disappearance of the absorption peak.

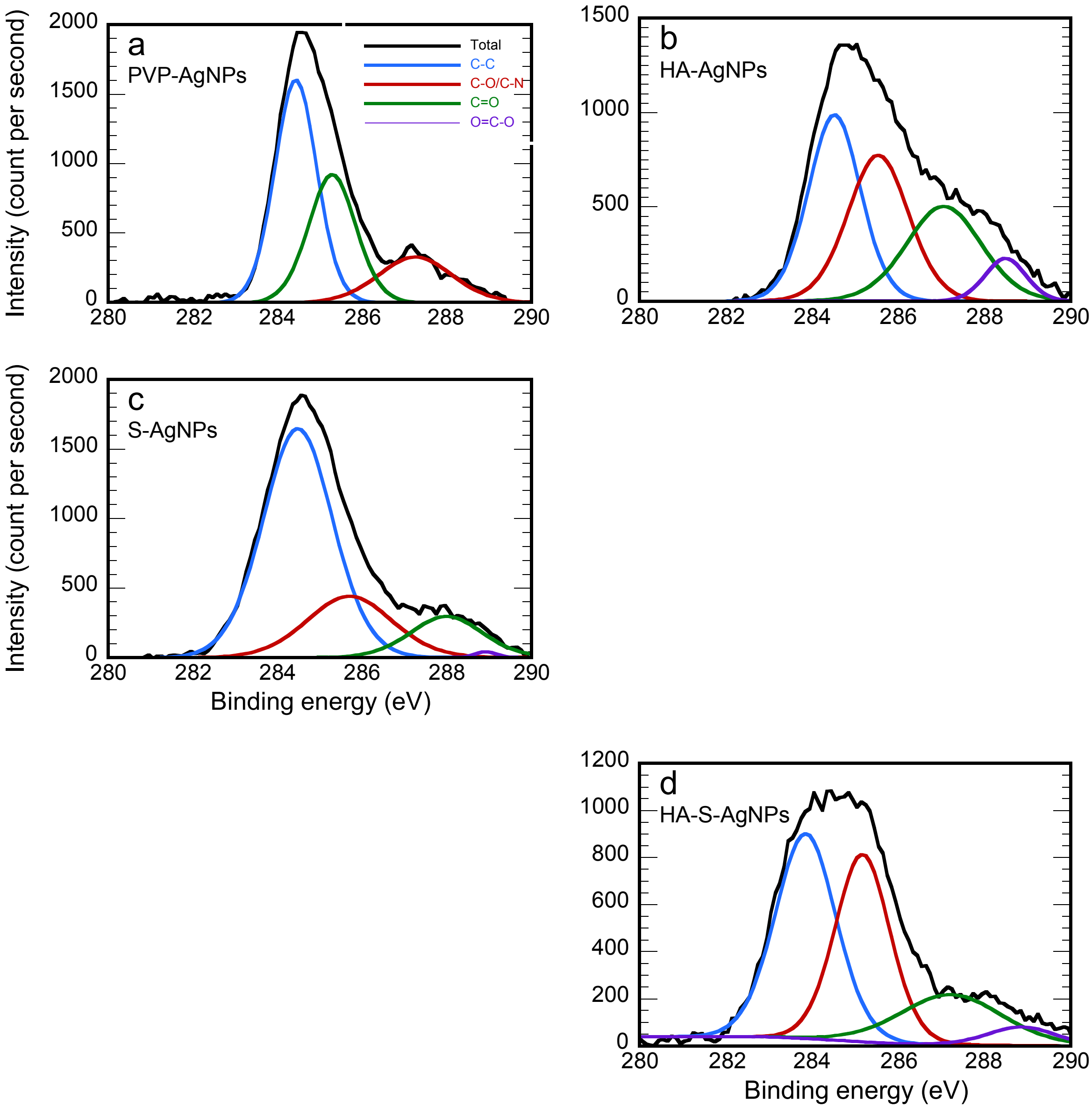

Figure S5. C 1s XPS experimental spectrum and the contribution of the fit of different AgNPs transformed in I=5 mM $Ca(NO_3)_2$.

Table S3. Composition (Percent of total carbon measured) of the total C 1s XPS spectra based on Lorentzian and Gaussian curve fitting after transformation in $Ca(NO_3)_2$.

Functional group	Binding Energy (eV)	PVP-AgNPs	HA-AgNPs	S-AgNPs	HA-S-AgNPs
C-C	284.5	46.68	35.36	65.83	42.93
C-N or C-O	285.6	34.34	32.36	21.48	35.32
C=O	287.5	18.84	25.91	12.19	17.50
O=C-O	288.6	0	6.37	0.50	4.25

Table S4. HDD (nm) during aggregation tests for PVP-AgNPs at pH 7±0.2 and a) I=10 mM with $NaNO_3$ with different environmental transformations.

Time (min)	PVP-AgNPs	HA-AgNPs	S-AgNPs	HA-S-AgNPs
0	82.5 ± 29.5	80.0 ± 33.5	86.3 ± 28.7	89.2 ± 24.0

10	87.1 ± 38.6	77.4 ± 30.7	88.2 ± 31.5	89.3 ± 32.0
30	84.1 ± 37.9	79.0 ± 36.8	88.3 ± 33.8	99.0 ± 31.8
60	81.2 ± 31.0	79.9 ± 36.8	88.7 ± 35.4	98.0 ± 59.1
120	80.4 ± 32.8	78.4 ± 33.0	89.4 ± 32.0	93.7 ± 66.3

Table S5. HDD (nm) during aggregation tests for PVP-AgNPs at pH 7±0.2 and a) I=10 mM with $Ca(NO_3)_2$ with different environmental transformations.

Time (min)	PVP-AgNPs	HA-AgNPs	S-AgNPs	HA-S-AgNPs
0	93.1 ± 38.5	86.0 ± 37.6	115.4 ± 47.6	100.1 ± 38.5
10	97.2 ± 43.4.6	99.2 ± 48.0	118.4 ± 53.5	126.2 ± 44.0
30	99.3 ± 43.4	148.7 ± 58.2	118.4 ± 50.7	141.0 ± 65.0
60	106.2 ± 43.1	177.4 ± 96.6	125.7 ± 56.0	145.3 ± 59.6
120	109.0 ± 42.6	244.2 ± 117.6	132.9 ± 56.4	164.3 ± 71.7

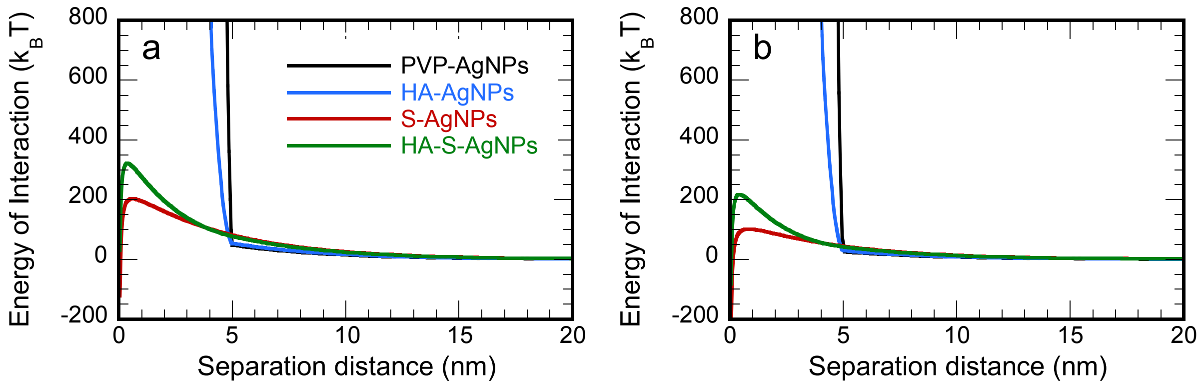

Figure S6. XDLVO energy of interaction in a) column filtration and b) QCM test at pH=7.0±0.2 and I=5 mM $NaNO_3$.The calculation was based on equations from Table S1 and vales of parameters from Table S2.

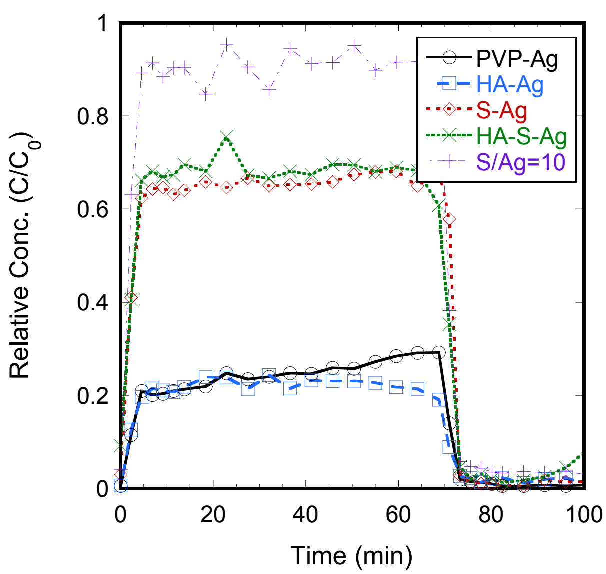

Figure S7. Breakthrough curve for the AgNPs transport in bare silica filter in column test at pH=7.0±0.2 and I=5 mM $NaNO_3$.

References

1 J. Gregory, *J. Colloid Interface Sci.*, 1975, **51**, 44–51.

2 J. Gregory, *J. Colloid Interface Sci.*, 1981, **83**, 138–145.

3 B. Vincent, J. Edwards, S. Emmett and A. Jones, *Colloids and Surfaces*, 1986, **18**, 261–281.

4 S. Lin and M. R. Wiesner, *Langmuir*, 2012, **28**, 15233–15245.

5 A. R. Petosa, D. P. Jaisi, I. R. Quevedo, M. Elimelech and N. Tufenkji, *Environ. Sci. Technol.*, 2010, **44**, 6532–6549.

6 O. Furman, S. Usenko and B. L. T. Lau, *Environ. Sci. Technol.*, 2013, **47**, 1349–1356.

7 A. O. Pinchuk, *J. Phys. Chem. C*, 2012, **116**, 20099–20102.

8 J. N. Israelachvili, *Intermolecular and Surface Forces*, Academic Press, London, Third., 2011.

9 J. W. Pavlik and E. M. Perdue, *Environ. Eng. Sci.*, 2015, **32**, 23–30.